

Impaired brain equanimity and neurogenesis in the diet-induced overweight mouse: a preventive role by syringic acid treatment

Amina Khatun, Titli Panchali, Sukhamoy Gorai, Ananya Dutta, Tridip Kumar Das, Kuntal Ghosh, Shrabani Pradhan, Keshab Chandra Mondal & Sudipta Chakrabarti

To cite this article: Amina Khatun, Titli Panchali, Sukhamoy Gorai, Ananya Dutta, Tridip Kumar Das, Kuntal Ghosh, Shrabani Pradhan, Keshab Chandra Mondal & Sudipta Chakrabarti (2023): Impaired brain equanimity and neurogenesis in the diet-induced overweight mouse: a preventive role by syringic acid treatment, *Nutritional Neuroscience*, DOI: [10.1080/1028415X.2023.2187510](https://doi.org/10.1080/1028415X.2023.2187510)

To link to this article: <https://doi.org/10.1080/1028415X.2023.2187510>



Published online: 22 Mar 2023.



Submit your article to this journal [↗](#)



View related articles [↗](#)



View Crossmark data [↗](#)



Impaired brain equanimity and neurogenesis in the diet-induced overweight mouse: a preventive role by syringic acid treatment

Amina Khatun^a, Titli Panchali^b, Sukhamoy Gorai^c, Ananya Dutta^b, Tridip Kumar Das^a, Kuntal Ghosh^a, Shrabani Pradhan^b, Keshab Chandra Mondal^d and Sudipta Chakrabarti ^a

^aDepartment of Biological Sciences, Midnapore City College, Paschim Medinipur, India; ^bDepartment of Paramedical & Allied Health Science, Midnapore City College, Paschim Medinipur, India; ^cDepartment of Neurological Sciences, Rush University Medical Center, Chicago, IL, USA; ^dDepartment of Microbiology, Vidyasagar University, Midnapore, India

ABSTRACT

Objectives: In this study mice were fed a high-fat diet for 12 weeks to establish diet-induced obesity and syringic acid (SA) was assessed for anti-obese, neuroprotective, and neurogenesis.

Method: Animals were given HFD for 12 weeks to measure metabolic characteristics and then put through the Barnes-maze and T-maze tests to measure memory. Additionally, the physiology of the blood–brain barrier, oxidative stress parameters, the expression of inflammatory genes, neurogenesis, and histopathology was evaluated in the brain.

Result: DIO raised body weight, BMI, and other metabolic parameters after 12 weeks of overfeeding. A reduced spontaneous alternation in behavior (working memory, reference memory, and total time to complete a task), decreased enzymatic and non-enzymatic antioxidants, oxidative biomarkers, increased neurogenesis, and impaired blood–brain barrier were all seen in DIO mice. SA (50 mg/kg) treatment of DIO mice (4 weeks after 8 weeks of HFD feeding) reduced diet-induced changes in lipid parameters associated with obesity, hepatological parameters, memory, blood–brain barrier, oxidative stress, neuroinflammation, and neurogenesis. SA also reduced the impact of malondialdehyde and enhanced the effects of antioxidants such as glutathione, superoxide dismutase (SOD), and total thiol (MDA). Syringic acid improved neurogenesis, cognition, and the blood–brain barrier while reducing neurodegeneration in the hippocampal area.

Discussion: According to the results of the study, syringic acid therapy prevented neurodegeneration, oxidative stress, DIO, and memory loss. Syringic acid administration may be a useful treatment for obesity, memory loss, and neurogenesis, but more research and clinical testing is needed.

KEYWORDS

Diet-induced overweight; syringic acid; PPAR- α ; blood–brain barrier; oxidative stress; neuroinflammation; neurogenesis; high fat diet

Introduction

Obesity and overweight have become major health problems worldwide. This happens due to the accumulation of excess body fat and leads to excessive body weight and body mass index (BMI) [1, 2]. According to the World Health Organization report (2019), obesity has roughly tripled today compared to the 1980s [3, 4]. Various genetic and environmental factors are responsible for the development of obesity and overweight [5–7]. Overweight and/or obesity can lead to many metabolic disorders such as hyperglycemia, insulin resistance, dyslipidemia, and livers with non-alcoholic fat deposits and are a consequence of chronic inflammation and oxidative stress [8–10]. Along with impaired metabolic balance and homeostasis, overweight and obesity can impair central nervous system (CNS) homeostasis, which is an important cause of

cognitive impairment and dementia [11–13]. A high-fat diet (HFD) fed to rodents has been reported to induce cognitive deficits [14, 15]. Inflammation and oxidative stress appear to be key factors contributing to blood–brain barrier leakage via reduced tight junction protein expression in the hippocampus among these cognitive dysfunctions [16–18]. In addition, other studies have found that HFD damages neurogenesis and brain plasticity [11]. Although obesity has been associated with CNS disorders, the mechanisms remain unclear. However, preventive and therapeutic approaches should be attempted to improve brain homeostasis and combat neurological degeneration due to obesity.

Due to their side effects, it is therefore always necessary to develop alternative drugs for the treatment of obesity-induced neurodegeneration. While numerous

polyphenolic compounds have been reported to have neuroprotective properties, syringic acid (SA) has almost never been explored. It has antioxidant, antimicrobial, antiendotoxic, and hepatoprotective properties. It acts as a free radical scavenger and helps reduce oxidative stress indicators [19].

SA, a naturally occurring polyphenol, is found in fruits, vegetables, and other plant products. A significant amount of SA is found in olives, dates, spices, squash, grapes, acai palm, honey, and red wine [19]. Plant polyphenols have been reported to exert various health benefits effects such as antioxidant, immunomodulatory, and anti-inflammatory properties. Little evidence suggests that polyphenols could be used to treat neurological diseases such as Alzheimer's and Parkinson's. SA had anti-obesity and anti-inflammatory properties [20]. However, the role of SA in obesity-induced neurodegeneration has not been studied to date. SA therapy can therefore be used to mitigate the effects of obesity-induced neurodegeneration. The aim of this investigation was to understand obesity-associated neurodegeneration and its control through the application of SA.

Materials and methods

Animals and ethics

Male adult BALB/c mice weighing (20 ± 3 g) were used in this study. Mice were acclimated under specified environmental conditions (temperature $32 \pm 2^\circ\text{C}$, light/dark cycle of 12 h, humidity $50 \pm 5\%$). A standard rodent diet (Hindustan Lever, Mumbai, India) was fed to the animals *ad libitum* along with sterile water. Animal studies were performed after obtaining approval from Vidyasagar University Institutional Animal Ethics Committee (ICE/7-09-2016, dated: 09/09/2016).

All animals were divided into three groups ($n = 3$) depending on the diet. Mice in group-I were treated as a control group (Ctrl) and received a conventional diet (22.3% protein, 13.5% fat, and 64.2% carbohydrate). To generate diet-induced obesity (DIO) in group-II mice, they were fed a high-fat diet (38.9% carbohydrate, 38.9% fat from lard, and 22.2% protein, total 22.3 KJ/g) for 12 weeks [21]. Group-III (DIOS) was fed the same high-fat diet for 12 weeks, with SA supplementation at 8 weeks for 4 weeks (SA was dissolved with 0.5% methylcellulose). The dosage of SA ($\geq 95\%$ HPLC, Sigma Aldrich, S6881) is 50 mg/kg body weight of mice [22]. Only 0.2 ml of 0.5% methylcellulose was orally administered to the Ctrl and DIO groups once a day for 4 weeks [21]. A regular meal was served to the control group once day. Syringic acid was administered

once a day to the DIOS group. All three groups (Ctrl, DIO, and DIOS) were adequately maintained throughout the course of treatment.

Bodyweight, BMI, and fasting blood glucose estimation

In this study, the final body weight of the mice were recorded along with weekly weight measurements. Body length was calculated using a vernier caliper to measure the nose-to-anal distance to within 0.1 mm (Central; model # 6420). Body mass index was calculated using the standard method, and the results were expressed in g/cm^2 [21, 23].

The mice were fasted the day before the blood glucose level was measured. According to the manufacturer's instructions, the Eco-Pack Glucose Estimation Kit (ACCUREX biomedical Pvt. Ltd, Mumbai, India) was used to assess the blood glucose level (mg/dl).

Blood collection for metabolic analyzes

Mice were sacrificed by cervical dislocation at the end of the experiment and different organs were removed and weighed. The orbital plexus was punctured to collect blood samples. For biochemical analysis, blood samples were centrifuged at 2,500 rpm for 20 min at 4°C collected the serum and stored at -20°C [21].

Blood lipid profile measurements

The ENZOPAK kit of cholesterol, triglyceride, LDL, HDL, VLDL, SGOT, and SGPT was used according to the manufacturer's protocol to measure cholesterol, triglycerides, LDL, HDL, VLDL, SGOT and SGPT in 1 μL of diluted plasma (Reckon Diagnostic p. Ltd, India).

Oil red O and hematoxylin and eosin staining

Following the recommended methodology, thawed liver and skin slices were rehydrated with 60 percent isopropanol and stained with Oil Red O (Sigma-Aldrich) followed by a 40 min of incubation. Nuclei were counterstained by soaking sections in Mayer's hematoxylin for 30 s. Finally, a mounting material was used to mount the section and then dehydrated them before coverslip [24]. Hematoxylin and eosin staining of brain sections was performed according to standard protocol [21].

Examining the permeability of the BBB

Evans Blue dye was used to measure BBB permeability and examine BBB physiology [25–27]. Mice were

given an intraperitoneal injection of a freshly made 10 μ L Evans Blue dye at 1% 1X PBS. Mice were given 10 min of rest before sacrifice. Then 4% PFA-PBS was used to fix the brains of the mice. An image of the brain was taken after the dissection [27].

Protein extraction and measurement

Brain tissue (hippocampus) was extensively homogenized using radioimmunoprecipitation assay buffer (RIPA). After 30 min incubation on ice, the samples were centrifuged at 10,000 rpm for 5 min. Then the supernatants were collected and stored at -20°C [28]. Protein concentration was measured using the Bradford Protein Assay Kit (Himedia, India).

Immunoblotting

For the immunoblot, a 25 μ g protein sample was electrophoresed by SDS-PAGE and blotted onto a nitrocellulose membrane (BioRad, china). The primary antibody was used in this study included β -actin (Abgenex, India 1:1000), IL1Ra (Affinity, UK; 1:1000), PPAR- α , and PCNA, (Santa Cruz Biotechnology, Santa Cruz, CA, USA; 1:1000). The membrane was then incubated for 1 h with HRP conjugated anti-mouse secondary antibody (Abgenex, India; 1:5000). Specific protein bands were detected with DAB [29].

Measurement of cerebral antioxidant activities

A Tissue Lyser II (Qiagen) was used to homogenize 8 mg of mouse brain tissue previously collected and stored at -20°C in Tris buffer (25mM Tris, 1mM EDTA, pH 7.4) to determine the enzyme activities. After centrifugation, the supernatant was subjected to enzymatic assay and protein quantification. The total protein concentration of the lysates was determined using the standard method.

According to the methods described by Patche et al., 15–20 g of protein lysates were used in the catalase activity experiment. Catalase activity was determined by resolving absorbance at 240 nm. Then, using a calibration standard curve the catalase concentration was calculated. International catalytic units/mg proteins were used to express catalase activity [30].

According to Dobi, et al., the cytochrome c reduction assay was used to determine total SOD activity. This process increases absorbance at 560 nm by reducing cytochrome c with superoxide radicals generated by the xanthine/xanthine oxidase system. Xanthine oxidase, 0.5mM xanthine, 0.2mM cytochrome c, 50mM KH_2PO_4 (pH 7.8), 2mM EDTA, and 1mM NaCN

were added to a 20 μ L aliquot of the lysates containing around 10 μ g of protein. Using a microplate reader (Robonik Readwell Touch Plate Analyzer), the reaction was monitored at 560 nm. Total SOD activity was calculated using an SOD calibration standard curve. The amount of SOD was expressed in international catalytic units/milligram protein and we restandardized the percentages against the criterion [31].

Malondialdehyde levels were determined using a thio-barbituric reactive substance assay [32] and reduced glutathione (GSH) was measured using the Ellman's reagent assay [33]. Total thiol concentration was measured using the molar extinction coefficient formula [34].

Where, $A_1 = (\text{Tris buffer} + \text{Homogenate})$, $A_2 = (\text{Tris buffer} + \text{Homogenate} + \text{DTNB})$ and $B = \text{DTNB only}$, $(1.07/0.05) = \text{total volume/sample volume}$ and $(13.6 \times 10^4) = \text{extinction coefficient}$.

Estimation of LDH (Lactate dehydrogenase)

The integrity of the synaptosomal layer was assessed monitoring of cytoplasmic LDH enzymatic activities. The enzymatic activity of LDH was assayed spectrophotometrically using an LDH test kit (Himedia, India). The absorbance was measured at different intervals. The one unit of action (U) determined as the oxidation result of 1 μ M NADH/min at 37°C .

Measurement of NO (Nitric oxide)

Using a NO kit (Himedia, India) and the Griess reagent 1.5 percent sulfanilamide in 1 mol/l HCl containing 0.15 percent N-(1-naphthyl) ethylenediamine dihydrochloride, the NO colorimetrically determined by staring at the nitrite in brain tissue homogenate. The nitrates were to be converted to nitrites, producing an intensely purple azo compound, and it was then examined at 540 nm.

Measurement of TNF- α and il1ra through elisa

As recommended by the manufacturers, TNF- α and IL1Ra concentrations were measured using commercially available mouse-specific Enzyme-Linked Immunosorbent Assay (ELISA) kits from Wuhan Fine Biotech Co., Ltd. in China. Concentrations were calculated using a plate reader system (Robonik readwell Touch ELISA Plate Analyzer).

RNA extraction and reverse transcription

Mice brains were removed from their skulls and stored at -80°C until the RNA could be extracted. RNA

extraction was also done from the experimental animal's liver. Tissue Lyser II (Qiagen, Chatsworth, CA) was used to grind brains and livers from control. DIO and DIOS mice. According to the manufacturer, RNA easy Mini Kit (HiPurA® Total RNA Miniprep Purification Kit, MB602) was used to extract the RNA from the brains and livers. Then, using MMLV reverse transcriptase and random hexamer primers (Hi-cDNA Synthesis Kit, MBT076), 2 µg of RNA was reverse transcribed into cDNA (Hi-cDNA Synthesis Kit, MBT076).

Gene expression analysis by qPCR

The tissues of interest were immediately prepared for semi qPCR. RNA extraction was carried out and then amplification was done by standard protocol [28, 35]. Using 2X PCR Taq Mixture (Himedia, India; MBT061) and particular mouse primers, the BIO-RAD T100 Thermal Cycler was used to conduct semi-quantitative PCR experiments. The expression of *iNOS*, *SOCS3*, *IL1Ra*, *NFκB*, and pro-inflammatory cytokine genes (*IL1β*, *IL6*, and *tnf-α*) was standardized against the *GAPDH* gene in brain lysate and *FAS*, *Leptin* and *PPAR-α* gene expression was standardized against *GAPDH* in liver tissue lysate. Table 1 provides a list of the primer sequences.

Microscopy

Images were captured using an Olympus CX21iLED microscope. Adobe Photoshop CS6 was used to adjust the brightness and contrast of the image.

Behavioral analysis

A total of 12 mice (from 3 separate experiments) were the subject of the behavioral study.

The Barnes maze test

The Barnes maze test was performed according to the operating procedure [36]. The Barnes Maze is a circular

platform 100 cm in diameter that is elevated 90 cm. It has a 5cm diameter escape hole that leads to a small space fitted under the platform. To divert attention from the true hole, there are 19 more false holes surrounding the maze. Although they do not lead to an escape chamber, the replica holes are similar to the escape hole. A 100 watt light bulb was used to illuminate the Maze. The mouse was put inside an opaque box in the center of the maze on the first day. The opaque box was taken out after ten seconds, and the mouse was manually led to the escape hole. After a quarter of an hour the first attempt began. In the first attempt, the mouse was left in the start box for another 10 seconds. Once released, the mouse had three minutes to locate the escape hole. The light was turned off as soon as the mouse spotted the opening. The mouse was left in the escape chamber for one minute before being returned to its housing cage. Animal performance was monitored by a video recording system. Each mouse was received four 15-minute learning attempts every day. The mouse was placed on the maze again during a probe session after four days of learning. This time the escape hole was sealed so it looked essentially like any other hole. Both the probe trial and the time spent at the escape hole were documented. We also considered how many additional holes were searched. The mouse was returned to its housing cage after 90 s [37].

T-maze

A simplified apparatus described elsewhere, was used for T-maze based memory tests [38]. Before testing, the mice were properly trained for 2 days. During the training period, mice were allowed to enter the right arm (food reward site) by blocking the left arm of the T-maze. After completion of the training, the mice were deprived of food overnight. After food deprivation, a final T-maze test was performed in which the mice entered either the left arm (negative turn) or the right arm (positive turn). Finally, the errors in the T-maze for identifying food reward sites were calculated.

Table 1. Mouse qPCR primer sequences of *GAPDH*, *IL6*, *IL10*, *nfkB*, *iNOS*, *PPAR α*, *FAS*, *Leptin*, *IL1-Ra*, *TNF α*, *IL-1β*

Gene	Forward primer (5'-3')	Reverse primer (5'-3')
IL6	TCAACTTCTCCAGCGTGATG	TCTTCCCTCTTTTCTCCTG
IL10	TCTCCGAGATGCCTTCAGACA	TCAGACAAGGCT TGGCAACCC A
NFκB	CGGCCACTGTAGTT GTG	TGCGTTCCGGTATAAGGTG
iNOS	CCCTCCGAAGTTTCTGGCAGCAGC	GGCTGTCA AGCCTCGTGGCTTTG
PPAR α	CCTGAACATCGAGTGTGGAATAT	GTTCTTCTTCTGAATCTTGACGT
FAS	TCCTGGAACGAGAACACGATCT	GAGACGTGTCACTCCTGGACT TG
Leptin	CAAGCAGTGCCTATCCAGA	AAGCCAGGAATGAAGTCCA
GAPDH	GGTGAAGGTCGGAGTCAACG	GTGAAGACGCCAGTGGACTC
IL1-Ra	GCAGCACAGGCTGGTGAATGA C	TGCCCCCGTGGATGCCCAAG
TNF α	TTCTGTCTACTGAACTTCGGGGTGATCGGTCC	GTATGAGAAGCAAATCGGCTGACGGTGTGGG
IL-1β	ATGGCAACTGTTCTGAACTCAAC T	CAGGACAGGTATAGATTCTTCTTT

Insilco docking studies

A computer docking and scoring study of the interaction of the compound with PPAR α - was performed using Auto Dock 4 (The Scripps Research Institute, La Jolla, USA) [38]. The crystal structure of PPAR α - (PDB code: 3VI8) was used for the docking experiment [39]. To generate apo protein, the ligand and water molecules were removed from the co-crystal structures and then processed by energy minimization [40]. For the docking run, 10 docking structures for the ligand were generated. The energetically preferred docked conformation was evaluated based on the Moledock and Re-Rank score. The docking poses were exported and examined with PyMOL software (The PyMol Molecular Graphics System, version 1.0r1, Schrödinger, LLC.).

Statistical analysis

Multiple comparison tests were used after one-way and two-way ANOVAs to carry out comparative studies between the groups. The error bars represent the mean \pm SD [41], and the *n* values represent the number of samples or animals used in each experiment. *P*-values < 0.05 were used to evaluate statistical significance (**p* < 0.05, ***p* < 0.01, ****p* < 0.001).

Results

Phenotypic and metabolic changes induced by DIO mice

Mice were fed an obese diet and a control diet for 12 weeks to create quickly and accurately a DIO model.

The influence of diet on BMI and body weight development was then examined. Compared to Ctrl, a significant increase in body weight was observed in DIO mice after the first week of the diet, which persisted through week 12 (Figure 1A,B). At week 12, the DIOS mice were larger than Ctrl mice, with a 50.84% increase in body weight compared to the Ctrl group (Figure 1A). On the other hand, the DIO mice showed a 105% increase in body weight compared to the Ctrl group. Furthermore, a significant increase in BMI was observed in the DIOS (44.30%) and DIO (104.87%) mice in contrast to the Ctrl mice after 12 weeks (Figure 1B). Blood triglyceride, cholesterol, LDL and VLDL levels were also measured and some significant changes were noted in DIO mice group compared to Ctrl group (Figure 2B–E), while in the DIO mice compared to the Ctrl group were found significantly lower blood HDL levels (Figure 2F). These results showed that a 12-week high-fat diet resulted in increases in body weight, BMI, and lipid profile. Numerous studies have already shown that overweight and obesity can lead to metabolic problems such as dysregulation of glucose and lipid metabolism, which can lead to fatty liver [8].

According to the model created for this study, DIO group had significantly higher fasting blood glucose levels (190%) than the Ctrl group (Figure 2A). Furthermore, the skin epidermal fat layer was significantly increased within the DIO group compared to the Ctrl group (Figure 2G). The expression of obesity-associated genes (*FAS*, *leptin* and *PPAR- α*) were assessed (Figure 3A–D). Significantly upregulated expression was found in the *FAS* (Figure 3B) and *leptin* gene

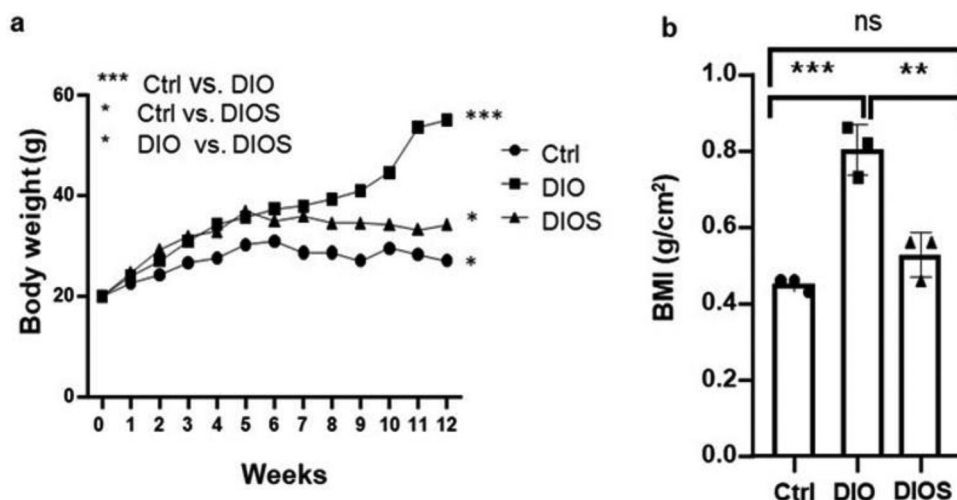


Figure 1. Diet induced obesity (DIO) causes an increase in body weight and BMI of the mice. (A) Graphs showing body weight measurements performed over the course of 12 weeks on mice treated with Ctrl, DIO, and DIOS. (B) At week 12, the body mass index (g/cm^2) was determined. Values are Mean \pm SD (*n* = 3), *n* = number of the mouse. Two-way ANOVA (A) and One-way ANOVA (B) followed by Tukey's multiple comparison test: **p* < 0.05, ***p* < 0.01, ****p* < 0.001.

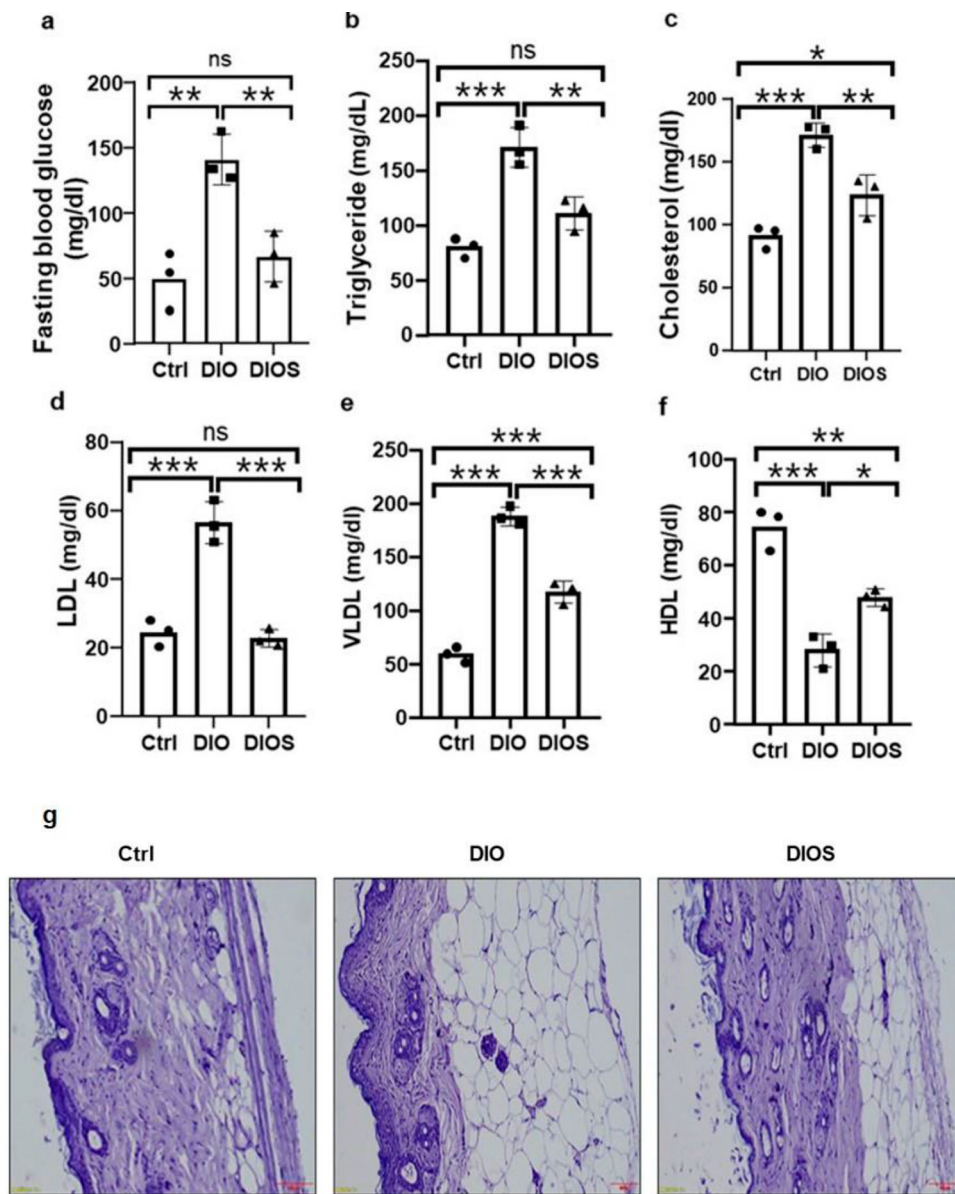


Figure 2. DIO results in increased fasting blood glucose levels and blood lipid profile (triglyceride, cholesterol, LDL & VLDL) except HDL, liver steatosis, SGOT, SGPT level, and skin histology in experimental mice. (A) Fasting blood glucose level in experimental animal, (B–F) Triglyceride, cholesterol, LDL, VLDL, and HDL level measurement at week 12 respectively in Ctrl, DIO, and DIOS group of mice. (G) skin histology of DIO-treated mice showed a very high level of lipid accumulation compared to Ctrl and DIO + syngic acid treated mice. These histological pictures are representative of the 3 mice studied. $n = 3$, The p values of $*p < 0.05$, $**p < 0.01$, $***p < 0.001$ were determined by one-way ANOVA followed by Tukey's multiple comparison test. Error bars correspond to the Mean \pm SD. The scale bar correspondence to 100 μ M (G).

(Figure 3C) in DIO mice compared to the Ctrl group of mice, while *PPAR- α* gene expression within the DIO group of mice compared to the Ctrl group was significantly downregulated (Figure 3D).

In addition, the liver of the DIO group showed accumulation of lipid (Figure 3G). To test this, slices of liver were stained with Oil Red O. The liver of DIO group showed an oil droplet-like structure indicative of lipid accumulation compared to the Ctrl group, showing that obese mice accumulate hepatic lipids. In the liver histology of the DIO mice, there were

differences in the intensity of liver oil red O staining. Taken together, these results indicated that by week 12, hepatic lipid and glucose metabolism was dysregulated in overfed mice. There were also significantly increased levels of SGOT and SGPT in the liver of the DIO group compared to the Ctrl group (Figure 3E,F). The changes obtained in the metabolic and phenotypic data in the DIO model strongly support the efficient development of the obesity model, resulting in dysregulation in lipid and glucose metabolism in the DIO group.

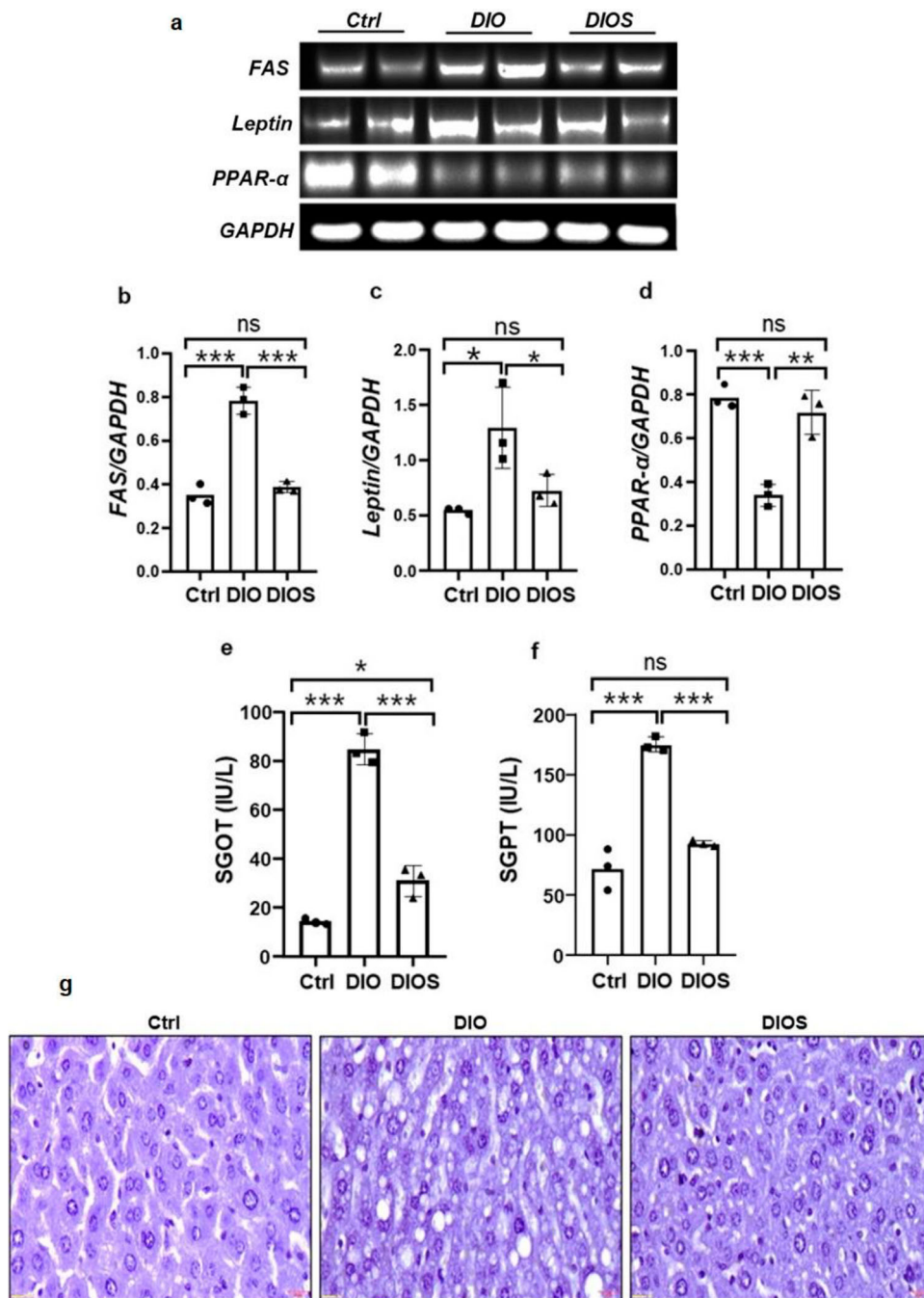


Figure 3. (A) Expression of obesity-associated genes in the liver by semi-q-PCR. (B)-(D) showed upregulation of genes (FAS, leptin, and PPAR- α) associated with obesity in DIO mice compared to Ctrl and DIOS mice. (E) & (F) showing SGOT and SGPT levels respectively at 12 weeks. (G) Oil Red O staining of the liver section in control mice showed no lipid accumulation, the staining of the livers of DIO mice revealed different levels of liver steatosis and lipid accumulation, but DIOS mice showed low levels of lipid accumulation in comparison with DIO mice. The histological images are representative of the 3 mice studied. $n = 3$, The p values of $*p < 0.05$, $**p < 0.01$, $***p < 0.001$ were determined by one-way ANOVA followed by Tukey's multiple comparison test. Error bars correspond to the Mean \pm SD. The scale bar correspondence to 20 μ M (G).

DIO induces blood brain barrier (BBB) leakage, oxidative stress and neuroinflammation

Obesity and other metabolic disorders are known to affect the BBB [42, 43], a critical interface that separates blood from CNS fluids and acts as a highly selective

barrier. BBB dysfunctions caused by obesity leads to a flow of substances into the brain, which then disrupts central homeostasis and can lead to increases in oxidative stress and inflammation in the brain. The DIO mouse used in this study had increased body weight

and BMI, and abnormal metabolism. Therefore, the consequences of high-fat diet on brain homeostasis have been studied. These effects included BBB physiology, neuroinflammation, oxidative stress and neurogenesis.

Evans Blue was injected intraperitoneally to study how DIO affects BBB physiology; this dye entered the bloodstream immediately. The blue color of the brains of the DIO mice indicated that overfeeding caused licking of the BBB, while the brains of the Ctrl mice remained white (Figure 4A). The effect of BBB leakage was studied by examining neuroinflammation and disrupted redox homeostasis. These phenomena have also been considered to be a consequence of obesity.

Next, a semi-qRt-PCR analysis was used to examine how high-fat diet affects neuroinflammation. The same trend was observed towards increased *il6*, *NFkB*, *il1β*, *iNOS* and *TNF-α* gene expression in the brain of DIO mice compared to Ctrl mice (Figure 4C–G). Furthermore, the anti-inflammatory *il1Ra* gene was significantly downregulated in the DIO group compared to the Ctrl mouse group (Figure 4H). These semi-quantitative RT-PCR results showed that DIO promotes neuroinflammation.

Redox homeostasis can be affected by the abnormalities in lipid and glucose metabolism observed in overfed animals. The uptake of this redox homeostasis is linked to the enzymatic antioxidant system. Catalase, SOD and antioxidant enzyme activity of GSH were examined in brain tissue lysate (Figure 5C–E). The content of catalase, superoxide dismutase and GSH was significantly reduced in the brain of the DIO mice compared to the group of Ctrl mice. While the concentration of MDA and total thiol was significantly increased in the brain tissue lysate of DIO mice compared to Ctrl mice (Figure 5A,B). This increased MDA and total thiol concentration and reduction in GSH, catalase and SOD activity led to an imbalance in redox status observed in DIO mice. Altered redox status in DIO mice decreased antioxidant activity, which may result in the formation of oxidized protein or lipid peroxidation products. It appears that high-fat diet appears to disrupt brain homeostasis and promotes BBB leakage, leading to oxidative stress and cerebral inflammation. A significant increase in LDH activities was detected in DIO mice compared to the Ctrl mice (Figure 5G). The brain lysate of the DIO mice showed a significantly increased NO level compared to the Ctrl mice (Figure 5F). In addition, TNF-α content (Figure 5H) was significantly increased in DIO mice compared to brain lysate from Ctrl mice, while IL1Ra content (Figure 5I) was significantly increased in DIO mice compared to Ctrl mice was reduced.

DIO impairs adult neurogenesis and behavioral activity

Adult neurogenesis can be hampered by BBB disruption and neuroinflammation. To study neuron proliferation in neurogenic niches, PCNA (Proliferating Cell Nuclear Antigen) protein expression was performed in experimental mouse brains (Figure 6D). A significant decrease in PCNA expression was observed in DIO mice compared to the Ctrl group, also there was a significant decrease in PPAR-α (Figure 6C) and IL1Ra (Figure 6B) protein expression. In addition, DIO mice showed disintegration within the hippocampal neuron compared to ctrl mice (Figure 6F). Next, we investigated how overfeeding might affect the behavior of mice, so we performed the memory test. Total time to complete the task in control and experimental animals was assessed using the barn maze and T-maze tests. The DIO groups took significantly longer than the Ctrl mice to complete the test (Figure 7A). The results of the behavioral study revealed by the Barns-maze test were performed to examine the working memory and reference memory error of experimental mice. With regard to memory, the respective time that mice need to reach the target whole was examined. In this study, DIO-induced mice showed a significant increase in the time needed to fully reach the target than the Ctrl mice. These results show that DIO mice showed lower spatial memory. The total number of entries for the target whole was examined in the working memory test. DIO mice showed a significant decrease in the frequency of entry into the target whole compared to Ctrl (Figure 7B).

Syringic acid treatment to prevent deleterious effect induced by DIO

Overfed mice appeared to be a suitable model to study how a high-fat diet affects weight gain and related problems. The DIOS mouse was treated with syringic acid once a day from the 8th week to the 12th week. It was confirmed by us that DIO mice without syringic acid showed a significant increase in body weight gain from week 1 to week 12 compared to Ctrl (Figure 1A). It is interesting to note that DIO + syringic acid (DIOS) did not significantly change body weight during weeks 1–7, but a significant reduction in body weight gain was noted at week 12 in the DIOS group (Figure 1A). At week 12, DIO mice show a significant increase in BMI compared to the DIOS group, but no significant increase was observed between the Ctrl and DIOS mice (Figure 1B). In addition, SA has shown remarkable preventive effects on DIO-induced elevated fasting blood

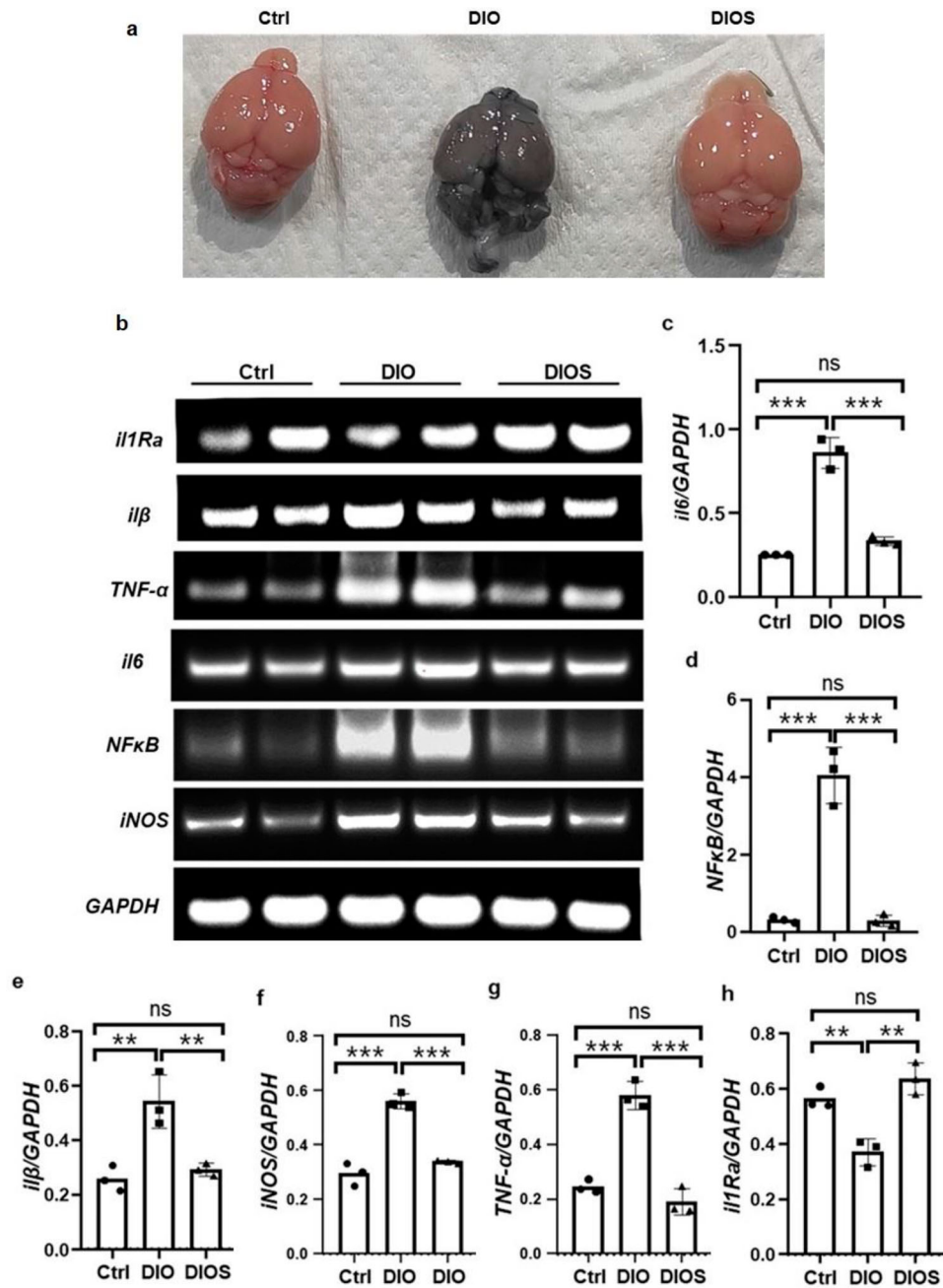


Figure 4. DIO induces BBB leakage and neuroinflammation. (A) Image shows the dorsal view of the Ctrl, DIO, and DIOS mice brains following injection with Evans blue dye. The blue dye was found in DIO mice compared to Ctrl while very less blue stain observed in DIOS mice but no blue stain found in Ctrl mice brains, it remains white ($n = 3$ brains). (B) Expression of inflammatory and anti-inflammatory cytokines by semi q-PCR. (C)–(H) qPCR expression of *NF-kB*, *il1β*, *il6*, *TNF-α*, *iNOS* and *il1Ra* genes in Ctrl and DIO, and DIOS mice. $n = 3$ One-way ANOVA followed by Tukey's multiple comparison test: ** $p < 0.01$, *** $p < 0.001$. The error bars are in relation to the Mean \pm SD.

glucose levels (Figure 2A). Also, the DIOS group significantly reduced blood triglyceride, cholesterol, LDL and VLDL levels (Figure 2B–E), while HDL levels increased significantly compared to the DIO mice group (Figure 2F). Side by side, DIOS mice also decreased subcutaneous fat deposition compared to DIO mice (Figure 2G).

Some other genes (*FAS* and *leptin*) associated with obesity were downregulated (Figure 3B,C), but *PPAR-α* (Figure 3D) was upregulated in DIOS mice compared to DIO mice. The DIOS group showed remarkable effects in preventing lipid deposition in the liver (Figure 3G) and also decreased SGOT and SGPT level (Figure 3E,F) compared to the DIO mouse group.

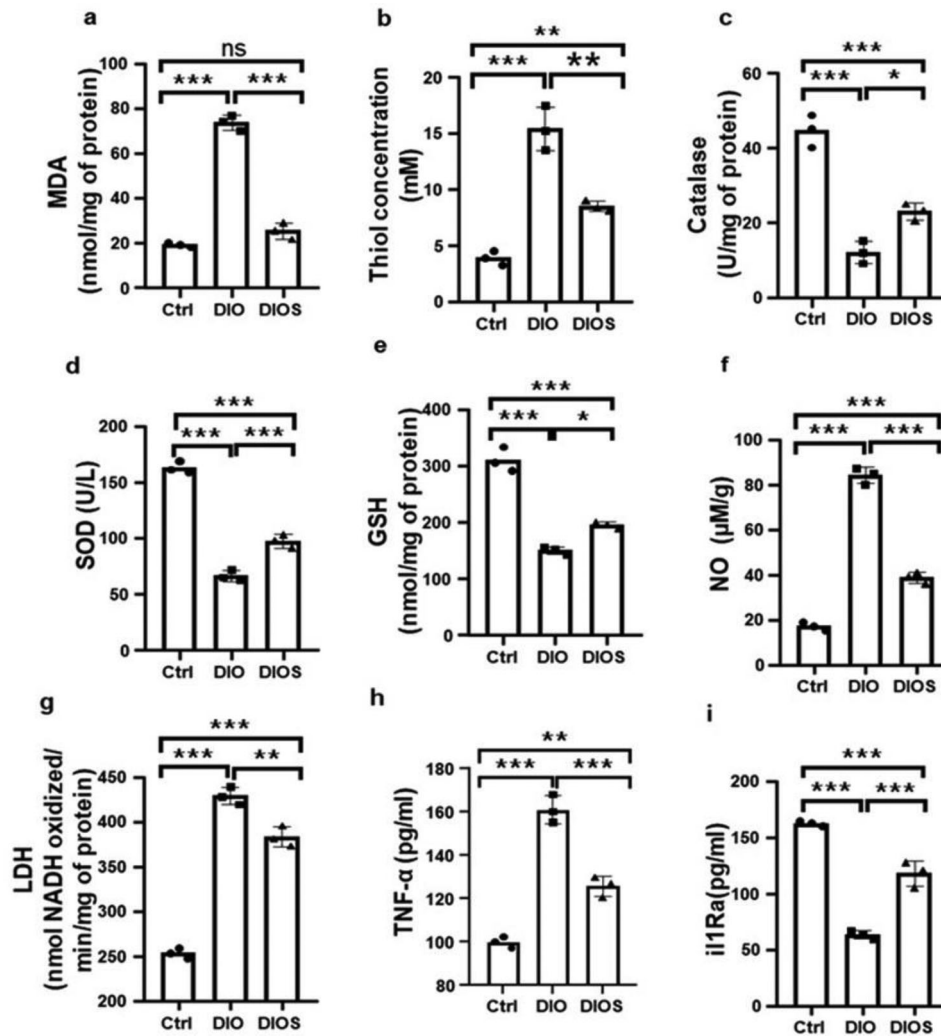


Figure 5. Effect of syringic acid on (A) MDA, (B) Thiol concentration, (C) Catalase, (D) SOD, (E) GSH, (F) NO, (G) LDH, (H) TNF- α , and (I) i11Ra of experimental animals. Antioxidant enzymes and activities were disrupted by DIO mice. $n = 3$ One-way ANOVA followed by Tukey's multiple comparison test: * $p < 0.05$, ** $p < 0.01$, *** $p < 0.001$. Error bars correspond to the Mean \pm SD.

Syringic acid prevents oxidative stress, BBB leakage, reduce neuroinflammation, and promotes neurogenesis

DIO disrupts central nervous system homeostasis by causing BBB leakage, oxidative stress and neurogenesis. Syringic acid has antioxidant properties that can reduce the effects of these disorders. The results of this study indicated that BBB leakage could be caused by DIO, while syringic acid (DIOS) treatment could limit BBB disruption (Figure 4A). Figure 4B shows the photographs of the qRt-PCR. However, neuroinflammation in the brain of DIOS appeared to be attenuated. Levels of several pro-inflammatory cytokines (i.e. *IL6*, *NF κ B*, *IL β* , *iNOS*, and *TNF- α*) were significantly reduced (Figure 4C–G), while expression of the *IL1Ra* gene (Figure 4H) was significantly increased in DIOS group

compared to the DIO group. In addition, some antioxidant enzymes (SOD, catalase, and GSH) were significantly increased in DIOS (Figure 5C–E) compared to DIO mice. It appeared that syringic acid-treated mice mitigated the harmful effects of free radicals by lowering MDA (Figure 5A) and total thiol (Figure 5B) concentrations in brain lysate compared to DIO. Syringic acid treatment also significantly reduced NO, LDH, and TNF- α levels (Figure 5F–H), respectively, while increasing IL1Ra levels (Figure 5I) in brain lysate compared to DIO mice.

The DIOS mouse group showed a significant increase in IL1Ra and PPAR α protein expression compared to the DIO mouse group (Figure 6B,C). In this study, it was also investigated whether syringic acid might have an impact on overfeeding-induced poor neurogenesis.

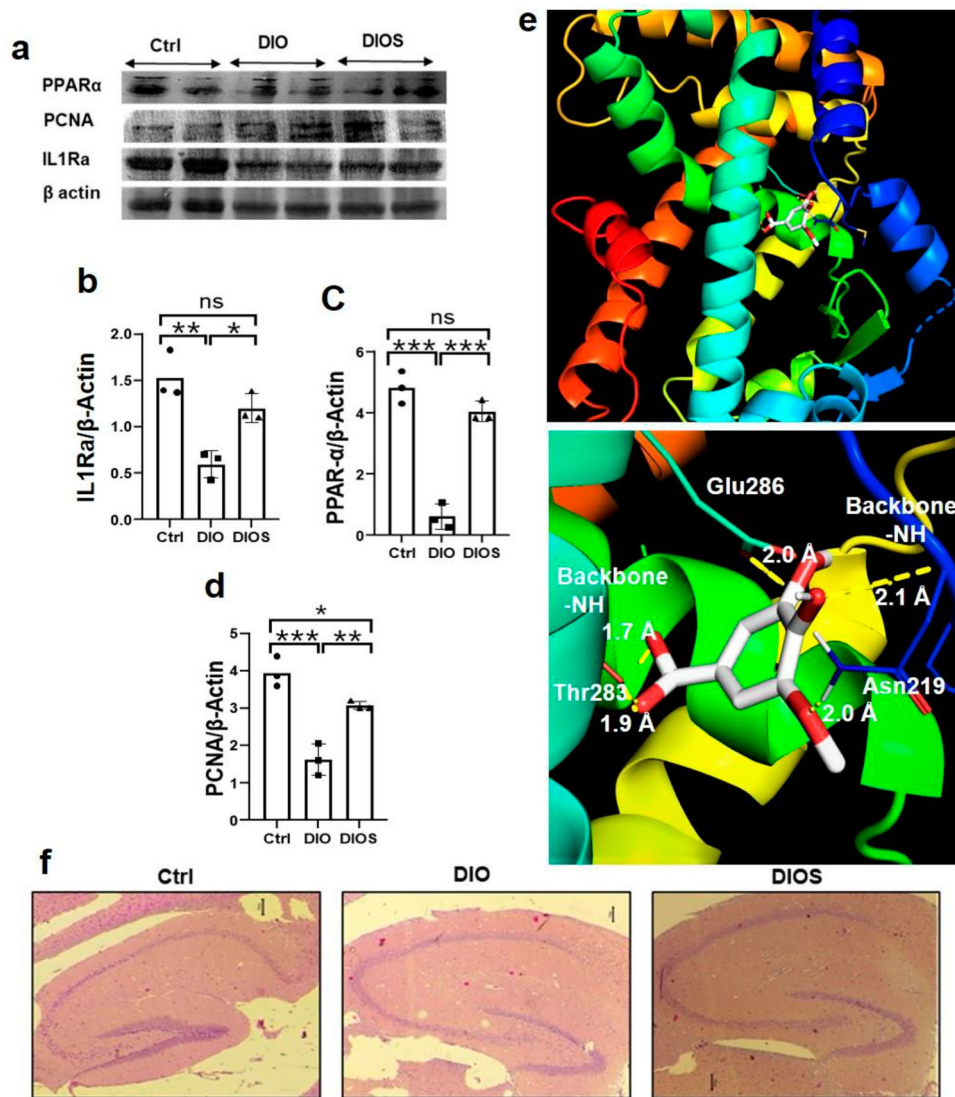


Figure 6. (A) Expression of proteins by western blot. (B)-(D) showed the expression of the proteins (il1Ra, PPAR- α , and PCNA) in experimental animals. (E) Model structure of syringic acid ligands docked to the ligand binding site of the PPAR- α protein. Residues involved in hydrogen-bonding are shown with dashed lines (yellow). (F) showed the HE staining of brains in experimental animals. These histological images are representative of the 3 mice studied. $n = 3$, One-way ANOVA followed by Tukey's multiple comparison test: * $p < 0.05$, ** $p < 0.01$, *** $p < 0.001$. Error bars correspond to the Mean \pm SD. The scale bar corresponds to 100 μ m (E).

PCNA protein expression was significantly increased in DIOS mice compared to DIO mice (Figure 6D). In brain histology, syringic acid treatment also improved hippocampal neurons compared to DIO mice (Figure 6F). According to this study, syringic acid can partially repair, regionally specific, poor neurogenesis caused by overnutrition. Supplementation of syringic acid in DIO-stimulated mice leads to restoration of spatial memory. The total number of entries to the target whole was examined in working memory. In this study, DIOS mice showed a marked increase in the number of entries into the intended whole compared to DIO mice (Figure 7A,B).

Molecular docking analysis

The animal model study based on high-fat diet showed that the compound syringic acid activates PPAR- α through ligand binding. The reported crystal structure of PPAR- α (PDB: 3VI8) in complex with phenyl propionic acid-type PPAR provides a detailed insight into the mode of ligand interactions within the binding pocket. More than 80% of the docking population revealed that syringic acid preferentially interacts with the PPAR- α through its ligand-binding site. The calculated in silico interaction energies between the ligand and the PPAR protein show a significantly negative value,

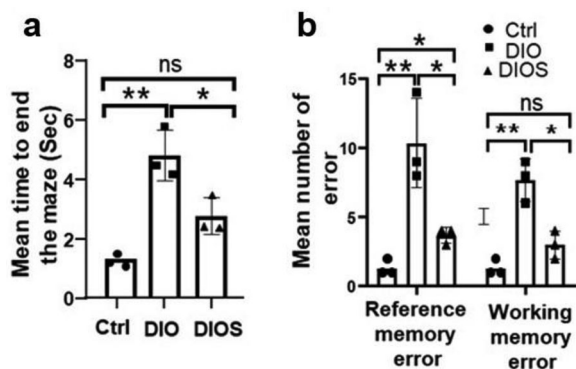


Figure 7. DIO increases the meantime and memory error in the maze test. (A) graph showing the increased mean time to complete the maze test in DIO mice compared to Ctrl and DIOS mice. (B) graph showing the working and reference memory error in Ctrl, DIO, and DIOS mice. $n = 3$ from 3 independent experiments. The p values of $*p < 0.05$, $**p < 0.01$, $***p < 0.001$ were determined by one-way ANOVA followed by Tukey's multiple comparison test. Error bars correspond to the Mean \pm SD.

indicating acceptable docking poses for additional analysis (Table 2). The docking poses demonstrated that the compound syringic acid could form hydrogen bonds with both side chain and backbone carbonyls/amide protons of PPAR- α through its ligand binding site (Figure 6E).

Discussions

In this study, young male BALB/c mice were fed a high-fat diet for 12 weeks to develop diet-induced obesity (DIO). By disrupting numerous metabolic parameters, the DIO model leads to a variety of metabolic problems, including increases in body weight, BMI and fasting blood glucose levels, and the onset of fatty liver. There were several DIO and/or HFD models that share similar metabolic impairments to those found in our study [21, 44–46]. According to previous research, overfeeding protocols with high-fat diets have been shown to promote visceral and/or subcutaneous adipocyte expansion in mice, leading to increases in body weight and BMI [21]. In our work, we choose to use a high-fat chow diet to enrich DIO mice.

We showed that body weight of DIO mice increased by 105% and body mass index (BMI) by 104.87% after

12th weeks of treatment compared to Ctrl mice (Figure 1). The increased body weight and BMI could be due to high-fat diets and thus accumulation of a larger amount of fat [47]. An increase in BMI and body weight was noted in high-fat diet induced mice with subcutaneous and/or visceral adipocyte development in mice [44–46].

In particular, obesity and overweight are known to be associated with elevated fasting blood sugar and type 2 diabetes, leading to fatty liver [48–51]. In this study, DIO mice showed significantly higher fasting blood glucose levels than Ctrl (Figure 2A; ~50 mg/dl in the Ctrl mouse group and ~145 mg/dl in the DIO mouse group) with fatty liver. Therefore, it can be speculated that hyperglycemia could promote chronic inflammation, insulin resistance and fatty liver in obesity [52–55].

It was found that hepatic *FAS* and *leptin* gene expression was upregulated in DIO mice compared to Ctrl (Figure 3). This can cause *FAS*-mediated hepatocyte apoptosis [56] and abnormality in food intake and energy expenditure due to *leptin* gene overexpression [57]. Hepatic *PPAR α* gene expression was reduced in DIO mice (Figure 3), which could lead to fatty liver development in mice with heterogeneous lipid accumulation in the form of water droplets in the liver (Figure 3d). Down-regulation of the hepatic *PPAR α* gene could promote lipogenesis and consequently contribute to the development of fatty liver [58].

After accounting for all effects, these data showed that the model established in this study is suitable for other DIO models. Furthermore, we found that DIO mice show similar pathologies as overweight and obese humans [59–61]. As a result, it supports its use in research on the negative effects of obesity on several physiological processes, including brain plasticity and homeostasis.

Several research findings have shown that obesity and overweight affect cognition and memory, neurogenesis and brain homeostasis [62–66]. A distinctive feature of these results is the fact that oxidative stress and inflammation have been shown to cause BBB dysfunction [67]. In the current study, we demonstrated that the brains of DIO mice exhibited higher levels of BBB leakage (Figure 4). It could be stimulated by inflammation and oxidative stress [68, 69]. Upregulation of the *NF κ B* gene and pro-inflammatory cytokines clearly indicated the neuroinflammatory states in the brain of DIO mice (Figure 4). Increased expression of pro-inflammatory genes and cytokines could be linked to the consequences of high glucose/high cholesterol in mice. Furthermore, these findings should be compared to the pure mammalian case in which obesity and/or a high-fat diet cause neuroinflammation

Table 2. Theoretically calculated interaction energy between ligand and PPAR- α .

Protein	Ligand	Binding energy (Kcal)	Interacting residues
PPAR- α	Syringic acid	-6.0	THR283:HG1 Glu286:OE1 Asn219:HD22 MET220:HN Ile317:HN

[70–72]. PPAR α and IL1R α protein expression was also downregulated in DIO mice (Figure 6).

Remarkably, in this experiment, DIO mice showed an increase in cerebral oxidative stress, which could lead to an increased accumulation of lipid peroxidation products in the brain (Figure 5). The regulation of oxidative stress can affect the differentiation and proliferation of progenitor cells as well as progenitor/stem cells of the brain [73–77]. We also showed that PCNA protein expression was downregulated in DIO mice (Figure 6). It concludes that the effect of high calorie consumption leads to neuronal damage in mice. Furthermore, overweight/obesity models based on genes

and/or diet have been found to exhibit reduced neural stem cell proliferation with very low formation of new born neurons [77–80]. Such reduced neurogenesis has also been demonstrated in hyperglycemia [81].

Further research is essential to define the effects of overfeeding on neuronal cell differentiation and survival in obese mice. Barnes maze test and T-maze test (Novel Object Recognition Test) clearly showed that cognitive abilities were impaired in DIO mice [14, 82] and the expression of many genes associated with antioxidant stress, neuronal activity and BBB functions [83, 84]. Therefore, we have shown in the same mouse model that overfeeding causes a range of negative

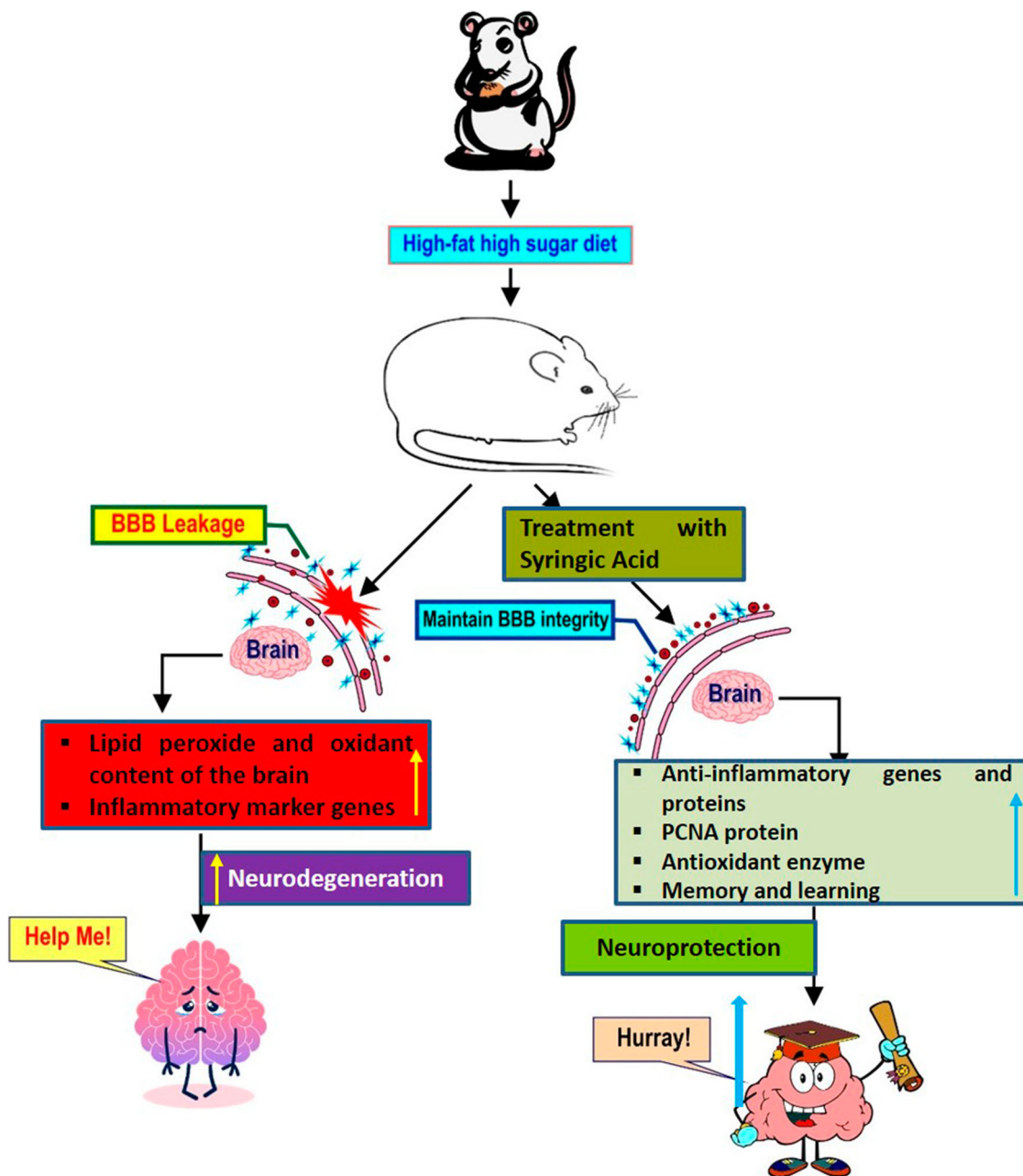


Figure 8. Summary of the study.

consequences for brain homeostasis, as evidenced by BBB leakage, neuroinflammation, increased oxidative stress and decreased neurogenesis. Furthermore, these results raise the question of which comes first – inflammation or oxidative stress? – which disrupts brain homeostasis and may help us understand how metabolic disorders can affect neurogenic activity and behavior. These results allow the exploration of the processes by which oxidative stress or inflammation caused by metabolic diseases disrupt neurogenic activity and behavior.

SA is a polyphenolic compound and has been found in many foods. We choose syringic acid because of its potential anti-inflammatory, antioxidant, anti-cancer and anti-diabetic effects. In DIOS mice, syringic acid not only improves metabolic parameters such as reduction of fatty liver and fatty tissue mass, but also reduces inflammatory factors and improves liver fat metabolism [20]. When we applied the syringic acid to the DIOS, a significant reduction in body weight and BMI was observed (Figure 1). Similarly, fasting blood glucose levels, total lipid profiles and epidermal skin fat deposition were significantly reduced in DIOS mice compared to the DIO mouse group and were probably close to the Ctrl group (Figure 2). Syringic acid has been shown to downregulate gene expression of *FAS* and *leptin* genes in the liver (Figure 3), which helps decrease lipogenesis and *FAS*-mediated hepatocyte apoptosis [57]. Syringic acid also upregulated the *PPAR- α* gene in the liver (Figure 3), which may increase lipid oxidation and prevent lipid accumulation in the liver just like the Ctrl group. A previous report showed that *PPAR- α* is activated by interacting with a common drug aspirin [58]. In silico docking analysis clearly showed that the syringic acid binds to the similar binding site of the *PPAR- α* suggesting that this interaction is vital for *PPAR- α* activation.

DIOS mice showed less lipid accumulation in the liver (Figure 3) and in parallel also lowered the levels of the liver markers SGOT and SGPT (Figure 3) as they increased oxidation, down-regulated lipid synthesis and finally reduced adipocyte cells thereby controlling obesity [20]. Given the low concentrations of these polyphenols, the effects of our study may not be as impressive as they could be. Pro-inflammatory and cytokine expression, BBB leakage, brain oxidative stress and memory function caused by DIO were all prevented in the DIOS group as well as in the Ctrl group (Figures 4, Figure 5, Figure 6 and Figure 7). The antioxidant properties of syringic acid could be associated with these protective effects [85, 86]. Surprisingly, DIO animals treated with syringic acid still show neurogenesis, although it appears to be less pronounced in virtually all hippocampal neurogenesis studies. In this way,

syringic acid was unable to fully protect neurons from neurogenic defects caused by DIO. Besides BBB leakage and oxidative stress, there may be other mechanisms that contribute to these neurogenic impairments. However, it could play the role in protecting the central nervous system in mice.

This study demonstrates how DIO adversely affects brain homeostasis and specifically brain neurogenesis. Despite overfeeding, syringic acid prevented significant weight gain in mice. We have developed a DIO protocol; it could be used as a novel physiological screening device to identify drugs that work against overweight or obesity. It will make it possible to find new ways to avoid weight gain and its adverse effects on the brain, such as oxidative stress, neuroinflammation, BBB leakage and poor neurogenesis. Syringic acid inhibits oxidative stress in the brain, BBB leakage, and improves neurogenesis, although it has minimal impact on body weight and corresponding BMI. It's possible that natural compounds can stop some neurological disorders caused by high-fat diet, but they don't have a major impact on body weight.

Conclusions

In mice, obesity induces BBB leakage, neuroinflammation, oxidative stress and neurodegeneration while decreasing neurogenesis. Obesity clearly had a negative impact on brain homeostasis. However, syringic acid not only alleviates obesity, but also lowers the adverse effects on the brain, such as oxidative stress, neuroinflammation, BBB leakage and poor neurogenesis. In silico-ligand-protein interaction reveals a very strong interaction between syringic acid and *PPAR- α* , which could play an important role in *PPAR- α* activation. Further, a detailed study is required to find out the mechanism of syringic acid. Figure 8 illustrates the summary of the study.

Acknowledgements

In order to complete this study, the Midnapore City College director, Dr. Pradip Ghosh, was acknowledged by the authors for providing all necessary assistance. As well, the authors would like to thank Mr. Abhishek Chakravarty, Department of Humanities, Midnapore City College, for meticulously editing the manuscript's English language. Conceptualization, S.C., A.K., S.G and K.G., Methodology, S.C., K.C.M., and A.K. Animal model work and histology, Supportive actions in performing the experiments: T.P., A.D., T.K.D., and S.P. Data Analysis, A.K., K.G., S.G., and S.C.; Writing – Original Draft, A.K, S.G., and S.C.; Writing – Review & Editing, S.C., S.G., and K.G.; Resources, A.K., S.G., K.G., S.P., K.C.M., and S.C.; Supervision, S.C.

Disclosure statement

No potential conflict of interest was reported by the author(s).

Funding

This study was supported by Indian Council of Medical Research (ICMR) Govt. of India 2021–11819 dated April 19, 2022. The authors acknowledged Dr. Pradip Ghosh, Director, Midnapore City College for his support.

Data availability statement

The authors confirm that the data supporting the findings of this study are available within the article.

Notes on contributors

Amina Khatun, M.Sc, exploring the obesity related neuronal disorder. She is working as a PhD student in Nutrition at Midnapore city College.

Titli Panchali M.Sc, exploring the obesity related disorder. She is working as a PhD student in Nutrition at Midnapore city College.

Sukhamoy Gorai PhD, exploring the neurodegeneration relation to small molecule development. He is working as a Post doctoral research fellow in the department of Neurological science, Rush University Medical center, Chicago, IL, USA.

Ananya Dutta M.Sc, exploring the nutrition research. She is working as a PhD student in Nutrition at Midnapore city College.

Tridip Kumar Das exploring the food research. He is working as a PhD student in Nutrition at Midnapore city College.

Kuntal Ghosh PhD, exploring the food research. He is working as an Assistant professor of microbiology at Midnapore city College.

Shrabani Pradhan PhD, exploring nutrition research. She is working as an assistant professor in Nutrition at Midnapore city College.

Keshab Chandra Mondal PhD, exploring food science research. He is working as a Professor of microbiology at Vidyasagar University.

Sudipta Chakrabarti PhD, exploring glial and neuronal cell signaling and neural stem cell differentiation with an emphasis to discover drugs and therapeutic strategies against neuroinflammatory and neurodegenerative disorders. He is working at Midnapore City College, Midnapore, West Bengal, India. He is working as a Principal and Associate professor of biological sciences at Midnapore city College.

ORCID

Sudipta Chakrabarti  <http://orcid.org/0000-0002-4867-160X>

References

- [1] Panuganti KK, Nguyen M, Kshirsagar RK, Doerr C. Obesity (nursing). StatPearls: StatPearls Publishing; 2021.
- [2] Ranasinghe C, Gamage P, Katulanda P, Andraweera N, Thilakarathne S, Tharanga P. A commentary on studies presenting projections of the future prevalence of dementia. BMC Public Health. 2013;13(1):1–8. doi:10.1186/1471-2458-13-1.
- [3] Fox A, Feng W, Asal V. Trade, investment and public health: compiling the evidence, assembling the arguments. Global Health. 2019;15(1):1–16.
- [4] Health AIo, Welfare. Overweight and obesity: an interactive insight. Australia: AIHW Canberra; 2019.
- [5] Romieu I, Dossus L, Barquera S, Blottière HM, Franks PW, Gunter M, et al. Energy balance and obesity: what are the main drivers? Cancer Causes Contr. 2017;28(3):247–58.
- [6] Albuquerque D, Nóbrega C, Manco L, Padez C. The contribution of genetics and environment to obesity. Br Med Bull. 2017;123(1):159–73.
- [7] Fonseca DC, Sala P, BdAM F, Reis J, Torrinhas RS, Bendavid I, et al. Body weight control and energy expenditure. Clin Nutr Exper. 2018;20:55–9.
- [8] Marsiglia L, Manti S, D'Angelo G, Nicotera A, Parisi E, Di Rosa G, et al. Oxidative stress in obesity: a critical component in human diseases. Intern J Mol Sci. 2015;16(1):378–400.
- [9] Gramlich Y, Daiber A, Buschmann K, Oelze M, Vahl C-F, Münzel T, et al. Oxidative stress in cardiac tissue of patients undergoing coronary artery bypass graft surgery: the effects of overweight and obesity. Oxid Med Cell Longev; 2018.
- [10] Godoy-Matos AF, Silva Júnior WS, Valerio CM. Curcumin analog A13 alleviates oxidative stress by activating Nrf2/ARE pathway and ameliorates fibrosis in the myocardium of high-fat-diet and streptozotocin-induced diabetic rats. Diabetol Metab Syndr. 2020;12(1):1–20.
- [11] Pugazhenth S, Qin L, Reddy PH. Common neurodegenerative pathways in obesity, diabetes, and Alzheimer's disease. Biochimica et Biophysica Acta (BBA)-Mol Basis Dis. 2017;1863(5):1037–45.
- [12] D O'Brien P, Hinder LM, Callaghan BC, Feldman EL. Neurological consequences of obesity. Lancet Neurol 2017;16(6):465-77.
- [13] Buie JJ, Watson LS, Smith CJ, Sims-Robinson C. Obesity-related cognitive impairment: The role of endothelial dysfunction. Neurobiol Dis. 2019;132:104580.
- [14] Corder ZA, Tamashiro KL. Developmental and environmental influences on physiology and behavior — 2014 Alan N. Epstein Research Award. Physiol Behav. 2015;152:508–71.
- [15] Cifre M, Palou A, Oliver P. α -Synuclein accumulation and GBA deficiency due to L444P GBA mutation contributes to MPTP-induced parkinsonism. Mol Neurodegener. 2018;13(1):1–14.
- [16] Davidson TL, Tracy AL, Schier LA, Swithers SE. A view of obesity as a learning and memory disorder. J Exper Psychol Anim Learn Cognit. 2014;40(3):261.
- [17] Sweeney MD, Sagare AP, Zlokovic BV. Blood–brain barrier breakdown in Alzheimer disease and other

- neurodegenerative disorders. *Nat Rev Neurol*. 2018;14(3):133–50.
- [18] Takata F, Nakagawa S, Matsumoto J, Dohgu S. Blood-brain barrier dysfunction amplifies the development of neuroinflammation: understanding of cellular events in brain microvascular endothelial cells for prevention and treatment of BBB dysfunction. *Front Cell Neurosci*. 2021;15:344.
- [19] Vo QV, Bay MV, Nam PC, Quang DT, Flavel M, Hoa NT, et al. Theoretical and experimental studies of the antioxidant and antinitrosant activity of syringic acid. *J Organ Chem*. 2020;85(23):15514–20.
- [20] Ham JR, Lee H-I, Choi R-Y, Sim M-O, Seo K-I, Lee M-K. Anti-steatotic and anti-inflammatory roles of syringic acid in high-fat diet-induced obese mice. *Food Funct*. 2016;7(2):689–97.
- [21] Pradhan S, Panchali T, Paul B, Khatun A, Jarapala R, Mondal S, C K, et al. Anti-obesity potentiality of Tapra fish (*Opisthopterus tardoore*) oil. *J Food Biochem*. 2020;44(11):e13448.
- [22] Zhao Y, Dang M, Zhang W, Lei Y, Ramesh T, Veeraraghavan VP, et al. Neuroprotective effects of Syringic acid against aluminium chloride induced oxidative stress mediated neuroinflammation in rat model of Alzheimer's disease. *J Funct Foods*. 2020;71:104009.
- [23] Ray M, Hor P, Ojha D, Soren J, Singh S, Mondal K. Bifidobacteria and its rice fermented products on diet induced obese mice: analysis of physical status, serum profile and gene expressions. *Benef Microb*. 2018;9(3):441–52.
- [24] Jung TS, Kim SK, Shin HJ, Jeon BT, Hahm JR, Roh GS. α -lipoic acid prevents non-alcoholic fatty liver disease in OLETF rats. *Liver Intern*. 2012;32(10):1565–73.
- [25] Kaya M, Ahishali B. Assessment of permeability in barrier type of endothelium in brain using tracers: Evans blue, sodium fluorescein, and horseradish peroxidase. *Permeability Barrier: Springer*; 2011. 369–82.
- [26] Yao L, Xue X, Yu P, Ni Y, Chen F. Evans blue dye: a revisit of its applications in biomedicine. *Contrast Media Mol Imag*. 2018;2018:7628037.
- [27] Saunders NR, Dziegielewska KM, Møllgård K, Habgood MD. Markers for blood-brain barrier integrity: how appropriate is Evans blue in the twenty-first century and what are the alternatives? *Front Neurosci*. 2015;9:385.
- [28] Chakrabarti S, Chandra S, Roy A, Dasarathi S, Kundu M, Pahan K. Upregulation of tripeptidyl-peptidase 1 by 3-hydroxy-(2,2)-dimethyl butyrate, a brain endogenous ligand of PPAR α : implications for late-infantile Batten disease therapy. *Neurobiol Dis*. 2019;127:362–73.
- [29] Bass JJ, Wilkinson DJ, Rankin D, Phillips BE, Szewczyk NJ, Smith K, et al. An overview of technical considerations for western blotting applications to physiological research. *Scand J Med Sci Sports*. 2017;27(1):4–25.
- [30] Patche J, Girard D, Catan A, Boyer F, Dobi A, Planesse C, et al. Diabetes-induced hepatic oxidative stress: a new pathogenic role for glycated albumin. *Free Rad Biol Med*. 2017;102:133–48.
- [31] Dobi A, Bravo SB, Veeren B, Paradela-Dobarro B, Álvarez E, Meilhac O, et al. Advanced glycation end-products disrupt human endothelial cells redox homeostasis: new insights into reactive oxygen species production. *Free Rad Res*. 2019;53(2):150–69.
- [32] Ohkawa H, Ohishi N, Yagi K. Assay for lipid peroxides in animal tissues by thiobarbituric acid reaction. *Anal Biochem*. 1979;95(2):351–8.
- [33] Elman G. Tissue sulfhydryl groups. *Arch Biochem Biophys*. 1959;82:70.
- [34] Nissankara Rao LS, Kilari EK, Kola PK. Protective effect of *Curcuma amada* acetone extract against high-fat and high-sugar diet-induced obesity and memory impairment. *Nutr Neurosci*. 2021;24(3):212–25.
- [35] Chakrabarti S, Roy A, Prorok T, Patel D, Dasarathi S, Pahan K. Aspirin up-regulates suppressor of cytokine signaling 3 in glial cells via PPAR α . *J Neurochem*. 2019;151(1):50–63.
- [36] Ye Q, Kim J. Loss of hfe function reverses impaired recognition memory caused by olfactory manganese exposure in mice. *Toxicol Res*. 2015;31(1):17–23.
- [37] Christakis DA, Ramirez JS, Ramirez J-M. Overstimulation of newborn mice leads to behavioral differences and deficits in cognitive performance. *Sci Rep*. 2012;2(1):1–6.
- [38] Morris GM, Huey R, Lindstrom W, Sanner MF, Belew RK, Goodsell DS, et al. Autodock4 and AutoDockTools4: automated docking with selective receptor flexibility. *J Comput Chem*. 2009;30(16):2785–91.
- [39] Kuwabara N, Oyama T, Tomioka D, Ohashi M, Yanagisawa J, Shimizu T, et al. Peroxisome proliferator-activated receptors (PPARs) have multiple binding points that accommodate ligands in various conformations: phenylpropanoic acid-type PPAR ligands bind to PPAR in different conformations, depending on the subtype. *J Med Chem*. 2012;55(2):893–902.
- [40] Gorai S, Bagdi PR, Borah R, Paul D, Santra MK, Khan AT, et al. Insights into the inhibitory mechanism of triazole-based small molecules on phosphatidylinositol-4, 5-bisphosphate binding pleckstrin homology domain. *Biochem Biophys Rep*. 2015;2:75–86.
- [41] Motulsky H. Prism 4 statistics guide—statistical analyses for laboratory and clinical researchers. San Diego (CA): GraphPad Software Inc; 2003:122–6.
- [42] Prasad S, Sajja RK, Naik P, Cucullo L. Diabetes mellitus and blood-brain barrier dysfunction: an overview. *J Pharmacovigil*. 2014;2(2):125.
- [43] Van Dyken P, Lacoste B. Impact of metabolic syndrome on neuroinflammation and the blood–brain barrier. *Front Neurosci*. 2018;12:930.
- [44] Marcelin G, Silveira ALM, Martins LB, Ferreira AV, Clément K. Deciphering the cellular interplays underlying obesity-induced adipose tissue fibrosis. *J Clin Investig*. 2019;129(10):4032–40.
- [45] Schoettl T, Fischer IP, Ussar S. Heterogeneity of adipose tissue in development and metabolic function. *J Exper Biol*. 2018;221(Suppl_1):jeb162958.
- [46] Caputo T, Tran VDT, Bararpour N, Winkler C, Aguilera G, Trang KB, et al. Anti-adipogenic signals at the onset of obesity-related inflammation in white adipose tissue. *Cell Mol Life Sci*. 2021;78(1):227–47.
- [47] Dhibi M, Brahmi F, Mnari A, Houas Z, Chargui I, Bchir L, et al. Chemopreventive effect of cactus *Opuntia ficus indica* on oxidative stress and genotoxicity of aflatoxin B1. *Nutr Metab (Lond)*. 2011;8(1):1–12.
- [48] Expert Panel on Detection E. Executive summary of the third report of the National Cholesterol Education

- Program (NCEP) expert panel on detection, evaluation, and treatment of high blood cholesterol in adults (adult treatment panel III). *JAMA: J Amer Med Assoc.* **2001**;285(19):2486–97.
- [49] Dharmalingam M, Yamasandhi PG. Nonalcoholic fatty liver disease and type 2 diabetes mellitus. *Ind J Endocrinol Metab.* **2018**;22(3):421.
- [50] Kang JH, Tsuyoshi G, Han IS, Kawada T, Kim YM, Yu R. Dietary capsaicin reduces obesity-induced insulin resistance and hepatic steatosis in obese mice Fed a high-fat diet. *Obesity.* **2010**;18(4):780–7.
- [51] Fappi A, Mittendorfer B. Different physiological mechanisms underlie an adverse cardiovascular disease risk profile in men and women. *Proc Nutr Soc.* **2020**;79(2):210–8.
- [52] Williams K, Shackel N, Gorrell M, McLennan S, Twigg S. Diabetes and nonalcoholic fatty liver disease: a pathogenic duo. *Endocr Rev.* **2013**;34(1):84–129.
- [53] Widjaja AA, Singh BK, Adami E, Viswanathan S, Dong J, Agostino D, A G, et al. Inhibiting interleukin 11 signaling reduces hepatocyte death and liver fibrosis, inflammation, and steatosis in mouse models of nonalcoholic steatohepatitis. *Gastroenterology.* **2019**;157(3):777–92. e14.
- [54] Cui A, Fan H, Zhang Y, Zhang Y, Niu D, Liu S, et al. Dexamethasone-induced Krüppel-like factor 9 expression promotes hepatic gluconeogenesis and hyperglycemia. *J Clin Investig.* **2019**;129(6):2266–78.
- [55] Matulewicz N, Karczewska-Kupczewska M. Insulin resistance and chronic inflammation. *Postepy Higieny i Medycyny Doswiadczalnej (Online).* **2016**;70:1245–58.
- [56] Li S, Zhao Y, He X, Kim T-H, Kuharsky DK, Rabinowich H, et al. Relief of extrinsic pathway inhibition by the Bid-dependent mitochondrial release of Smac in Fas-mediated hepatocyte apoptosis. *J Biol Chem.* **2002**;277(30):26912–20.
- [57] Chakrabarti S, Prorok T, Roy A, Patel D, Dasarathi S, Pahan K. Upregulation of IL-1 receptor antagonist by aspirin in glial cells via peroxisome proliferator-activated receptor- α . *J Alzheimer's Dis.* **2021**;5(1):647–661. (Preprint).
- [58] Izquierdo AG, Crujeiras AB, Casanueva FF, Carreira MC. Leptin, obesity, and leptin resistance: where are we 25 years later? *Nutrients.* **2019**;11(11):2704.
- [59] Kohjima M, Enjoji M, Higuchi N, Kato M, Kotoh K, Yoshimoto T, et al. Re-evaluation of fatty acid metabolism-related gene expression in nonalcoholic fatty liver disease. *Int J Mol Med.* **2007**;20(3):351–8.
- [60] Manojan K, Benny P, Bindu A. Prevalence of obesity and overweight among medical students based on new Asia-Pacific BMI guideline. *Kerala Med.* **2019**;12(1):13–5.
- [61] Schutz DD, Busetto L, Dicker D, Farpour-Lambert N, Pryke R, Toplak H, et al. European practical and patient-centred guidelines for adult obesity management in primary care. *Obes Facts.* **2019**;12(1):40–66.
- [62] Bracke A, Domanska G, Bracke K, Harzsch S, van den Brandt J, Bröker B, et al. Obesity impairs mobility and adult hippocampal neurogenesis. *J Exp Neurosci.* **2019**;13:1179069519883580.
- [63] Kaptan Z, Akgün-Dar K, Kapucu A, Dedeakayogulları H, Batu Ş, Üzümlü G. Long term consequences on spatial learning-memory of low-calorie diet during adolescence in female rats; hippocampal and prefrontal cortex BDNF level, expression of NeuN and cell proliferation in dentate gyrus. *Brain Res.* **2015**;1618:194–204.
- [64] Parimisetty A, Dorsemans A-C, Awada R, Ravanan P, Diotel N, Lefebvre d'Hellencourt C. Non-alcoholic fatty liver disease induces signs of Alzheimer's disease (AD) in wild-type mice and accelerates pathological signs of AD in an AD model. *J Neuroinflamm.* **2016**;13(1):1–13.
- [65] Nguyen JC, Killcross AS, Jenkins TA. Obesity and cognitive decline: role of inflammation and vascular changes. *Front Neurosci.* **2014**;8:375.
- [66] Alam MJ, Kitamura T, Saitoh Y, Ohkawa N, Kondo T, Inokuchi K. Adult neurogenesis conserves hippocampal memory capacity. *J Neurosci.* **2018**;38(31):6854–63.
- [67] Tabassum S, Misrani A, Yang L. Exploiting common aspects of obesity and Alzheimer's disease. *Front Hum Neurosci.* **2020**;14:602360.
- [68] Roh H-T, Cho S-Y, So W-Y. Obesity promotes oxidative stress and exacerbates blood-brain barrier disruption after high-intensity exercise. *J Sport Health Sci.* **2017**;6(2):225–30.
- [69] Kalkman HO. The association between vascular inflammation and depressive disorder. causality, biomarkers and targeted treatment. *Pharmaceuticals.* **2020**;13(5):92.
- [70] Ghaddar B, Veeren B, Rondeau P, Bringart M, Lefebvre d'Hellencourt C, Meilhac O, et al. Re-epithelialization and immune cell behaviour in an ex vivo human skin model. *Sci Rep.* **2020**;10(1):1–17.
- [71] Tchang BG, Saunders KH, Igel LI. Best practices in the management of overweight and obesity. *Med Clin.* **2021**;105(1):149–74.
- [72] Kim JD, Yoon NA, Jin S, Diano S. Microglial UCP2 mediates inflammation and obesity induced by high-fat feeding. *Cell Metab.* **2019**;30(5):952–62. e5.
- [73] Agudelo LZ, Ferreira DM, Cervenka I, Bryzgalova G, Dadvar S, Jannig PR, et al. Kynurenin acid and Gpr35 regulate adipose tissue energy homeostasis and inflammation. *Cell Metab.* **2018**;27(2):378–92. e5.
- [74] Albadri S, Naso F, Thauvin M, Gauron C, Parolin C, Duroure K, et al. Redox signaling via lipid peroxidation regulates retinal progenitor cell differentiation. *Develop Cell.* **2019**;50(1):73–89. e6. e6.
- [75] Muñoz MF, Argüelles S, Marotta F, Barbagallo M, Cano M, Ayala A. Effect of age and lipoperoxidation in rat and human adipose tissue-derived stem cells. *Oxid Med Cell Longev.* **2020**;2020:6473279.
- [76] Chaudhari P, Ye Z, Jang Y-Y. Roles of reactive oxygen species in the fate of stem cells. *Antiox Redox Signal.* **2014**;20(12):1881–90.
- [77] Purkayastha S, Cai D. Disruption of neurogenesis by hypothalamic inflammation in obesity or aging. *Rev Endocr Metab Disord.* **2013**;14(4):351–6.
- [78] Bailey AP, Koster G, Guillermier C, Hirst EM, MacRae JI, Lechene CP, et al. Antioxidant role for lipid droplets in a stem cell niche of *Drosophila*. *Cell.* **2015**;163(2):340–53.
- [79] Sudhakar V, Richardson RM. A New Era for surgical neurotherapeutics. *Neurotherapeutics.* **2019**;16(1):1–75.
- [80] Park HR, Park M, Choi J, Park K-Y, Chung HY, Lee J. A high-fat diet impairs neurogenesis: involvement of lipid peroxidation and brain-derived neurotrophic factor. *Neurosci Lett.* **2010**;482(3):235–9.

- [81] McNay DE, Briançon N, Kokoeva MV, Maratos-Flier E, Flier JS. Remodeling of the arcuate nucleus energy-balance circuit is inhibited in obese mice. *J Clin Investig.* **2012**;122(1):142–52.
- [82] Ho N, Sommers MS, Lucki I. Effects of diabetes on hippocampal neurogenesis: links to cognition and depression. *Neurosci Biobehav Rev.* **2013**;37(8):1346–62.
- [83] Gawel K, Gibula E, Marszalek-Grabska M, Filarowska J, Kotlinska JH. Assessment of spatial learning and memory in the barnes maze task in rodents—methodological consideration. *ArchPharmacol.* **2019**;392(1):1–18.
- [84] Yabluchanskiy A, Tucsek Z, Hertelendy P, Sonntag WE, de Cabo R, Farkas E, et al. Nrf2 deficiency exacerbates obesity-induced oxidative stress, neurovascular dysfunction, blood–brain barrier disruption, neuroinflammation, amyloidogenic gene expression, and cognitive decline in mice, mimicking the aging phenotype. *J. Gerontol.* **2018**;73(7):853–863.
- [85] Yan Q, Zhang H, Hui K, Shao Q. Family history is related to high risk of recurrent events after ischemic stroke or transient ischemic attack. *J Stroke Cerebrovasc Dis.* **2022**;31(1):106151.
- [86] Tanaka T, Iwamoto K, Wada M, Yano E, Suzuki T, Kawaguchi N, et al. Dietary syringic acid reduces fat mass in an ovariectomy-induced mouse model of obesity. *Menopause.* **2021**;28(12):1340–50.